



## Relationships between lightning and properties of convective cloud clusters

Joanna M. Futyán<sup>1,2</sup> and Anthony D. Del Genio<sup>2</sup>

Received 30 March 2007; revised 23 June 2007; accepted 5 July 2007; published 8 August 2007.

[1] Satellite observations of convective system properties and lightning flash rate are used to investigate the ability of potential lightning parameterizations to capture both the dominant land-ocean contrast in lightning occurrence and regional differences between Africa, the Amazon and the islands of the maritime continent. As found in previous studies, the radar storm height is tightly correlated with the lightning flash rate. A roughly second order power-law fit to the mean radar echo top height above the 0°C isotherm is shown to capture both regional and land-ocean contrasts in lightning occurrence and flash rate using a single set of parameters. Recent developments should soon make it possible to implement a parameterization of this kind in global models. Parameterizations based on cloud top height, convective rain rate and convective rain fraction all require the use of separate fits over land and ocean and fail to capture observed differences between continental regions.

**Citation:** Futyán, J. M., and A. D. Del Genio (2007), Relationships between lightning and properties of convective cloud clusters, *Geophys. Res. Lett.*, 34, L15705, doi:10.1029/2007GL030227.

### 1. Introduction

[2] Knowledge of the distribution of lightning around the globe is important in many fields. Lightning is an important source of nitrogen oxides in the tropical upper troposphere, influencing ozone production and the oxidizing capacity of the atmosphere [Stockwell *et al.*, 1999]. Lightning strikes are also the dominant cause of wild fires in remote regions [Stocks *et al.*, 2002], providing a source of biomass burning aerosol and influencing the carbon cycle. The ability to predict lightning occurrence in climate models (GCMs) is therefore a valuable tool in understanding how these impacts may change in the future. In addition, lightning is a tracer of vigorous convection that can be measured with relative ease from satellite [Christian, 1999], and hence provides a valuable means of validating the performance of model convective schemes [e.g., Del Genio *et al.*, 2007].

[3] To first order, lightning occurs where vigorous convective updrafts loft large particles above the 0°C isotherm [Williams, 2005, and references therein], although aerosol effects may modulate this picture, with less lightning observed over ocean even for storms with comparable radar signatures [Cecil *et al.*, 2005]. Existing lightning parameterizations use the height of deep convective clouds [Price and

Rind, 1992; Michalon *et al.*, 1999] or the convective rain rate [Meijer *et al.*, 2001; Allen and Pickering, 2002] as proxies for the intensity of convection. As these variables show only weak contrasts between continental and oceanic regions, separate parameterizations are required to capture the observed two order of magnitude differences in lightning frequency [Orville and Henderson, 1986; Boccippio *et al.*, 2000]. Parameterizations based on the convective mass flux have also been proposed [Grewe *et al.*, 2001; Allen and Pickering, 2002], but these cannot be directly validated observationally.

[4] Price and Rind [1992] and Michalon *et al.* [1999] suggest parameterizations based on observations of a fifth order power law relationship between radar echo top height and lightning flash rate over the continental US [Williams, 1985]. However, in developing the parameterizations, the fifth order dependence was assumed to apply to the cloud top height (as this was all that was available from GCMs), rather than the radar echo top height. This may not be appropriate in all regions, as the cloud top may be several kilometers higher than the height to which significant radar signal extends, especially over ocean [Liu *et al.*, 2007]. In fact, the cloud top height (height to which small particles extend) is often a poor tracer of the intensity of the convection that produced it. In some cases, the atmosphere may be unstable to great depths, allowing deep clouds to develop, but only weakly buoyant, supporting only weak updrafts. This is often the case over oceanic regions, while over land large positive buoyancy often drives vigorous convection [Lucas *et al.*, 1994; Liu *et al.*, 2007]. Cloud heights are therefore similar in deep convective regions over land and ocean, despite large contrasts in convective vigor.

[5] Radar instruments provide an estimate of the height to which large particles are lifted by the convective updraft. This is more directly related to the intensity of convection than the cloud height, with observations of significant radar echo in the mixed phase region of the cloud being well correlated with lightning occurrence [Williams *et al.*, 1992; Zipser and Lutz, 1994]. Ushio *et al.* [2001] further quantified this relationship using TRMM (Tropical Rainfall Measuring Mission) precipitation radar (PR) and lightning imaging sensor (LIS) data, reproducing Williams' [1985] fifth order relationship over the US, and confirming that similar relationships hold in other regions, although with some variation in the power law slope.

[6] Recently, it has become possible to infer cumulus scale updraft velocities in GCMs [Sud and Walker, 1999; Donner *et al.*, 2001; Del Genio *et al.*, 2007]. Combined with information about the size distribution of hydrometeors and fallspeeds within the cumulus updraft, it will soon be possible to diagnose the vertical profile of large hydrometeors in GCMs. We therefore wish to revisit the question

<sup>1</sup>Department of Applied Physics and Applied Mathematics, Columbia University, New York, New York, USA.

<sup>2</sup>NASA Goddard Institute for Space Studies, New York, New York, USA.

**Table 1.** Definition of Analysis Regions<sup>a</sup>

Region	Longitude Range	Latitude Range	Surface Type	Season
Africa	20°W–50°E	20°S–30°N	land only	Jun–Sept 2005 (FD07), Jun–Aug 2004 (ISCCP)
Atlantic	50°W–20°E	10°S–20°N	ocean only	Jun–Sept 2005 (FD07), Jun–Aug 2004 (ISCCP)
Amazon	40–80°W	20°S–10°N	land only	Dec 2004–Feb 2005
West Pacific	110–180°E	20°S–20°N	ocean only	Dec 2004–Feb 2005
Maritime continent	110–180°E	20°S–20°N	land and coastal	Dec 2004–Feb 2005

<sup>a</sup>FD07 refers to the *Futyán and Del Genio* [2007] dataset, and ISCCP to that created here using ISCCP and TRMM data.

of how best to parameterize lightning in climate models and to assess the potential of radar height based relationships for this task.

[7] Existing relationships [*Williams, 1985; Ushio et al., 2001*] do not provide all of the information required to develop a radar height based parameterization as they relate the radar height and flash rate at the scale of individual convective cells (rather than the ensemble of cells represented in any GCM grid-box) and exclude non-flashing convection. Here, we use TRMM PR, LIS and ISCCP (International Satellite Cloud Climatology Project) data to examine the behaviour at the more comparable convective cluster scale. Systems where no lightning is observed are included to ensure an unbiased estimate of the frequency of occurrence of lightning. Fits are made to the observed relationships for each variable of interest and their predictive capability is assessed based on the ability to capture both the dominant land-ocean contrast in lightning occurrence, and the regional contrast between the Amazon and Africa [*Boccippio et al., 2000*].

## 2. Methodology

[8] As described by *Futyán and Del Genio* [2007] (hereinafter referred to as FD07), convective cloud clusters were identified as contiguous regions of cold cloud cover in GERB (Geostationary Earth Radiation Budget)-like thermal

flux data derived from Meteosat-7 narrowband data. Radar and lightning properties were obtained from coincident (within 30 minutes) PR and LIS data by matching the systems to TRMM overpasses. FD07 matched properties for over 1500 systems in the African/Atlantic region, which we use here to fit the observed dependence of lightning flash rate on various system properties.

[9] To test the predictive ability of these fits, we created comparable datasets for various regions of interest. ISCCP infra-red brightness temperature data were used to identify cloud clusters in these regions (as GERB-like data are limited to the African/Atlantic domain), which were then matched to coincident TRMM overpasses (also within 30 minutes) as in FD07. The ISCCP brightness temperature data were smoothed onto a regular 0.5° grid to provide comparable resolution to the data used by FD07 and one month of concurrent data was used to determine appropriate narrowband thresholds for system identification.

[10] As LIS provides view-time information on a 0.5° grid, flash rates were calculated at this resolution. The flash rate was found for all grid boxes in a given system with greater than 80% area coverage by PR. Flash rates were normalized by the area of deep convection in each grid-box and averaged over all grid boxes where deep convection occurred within the system. This provides an estimate of the average number of flashes per minute per unit convective rain area for that system.

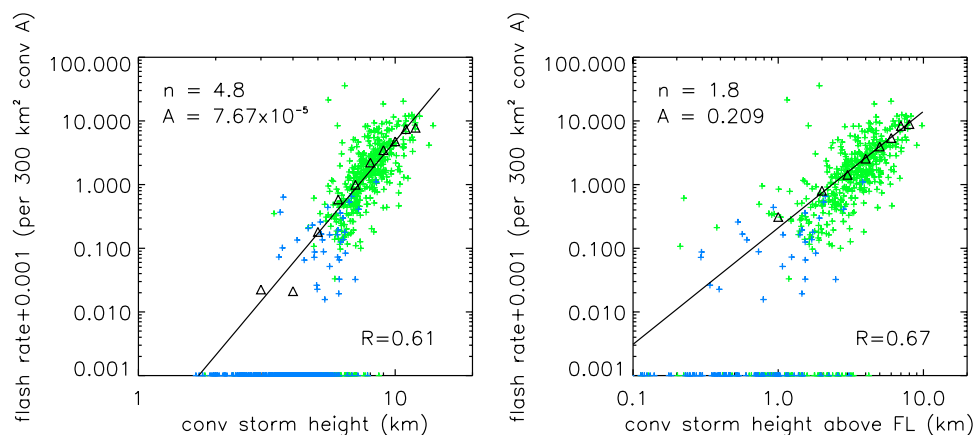


**Figure 1.** Scatterplot of the flash rate per unit convective area (left) against the mean convective radar storm height and (right) against the height of penetration of convective echos above the 0°C isotherm. Data are from 4 months of observations over the African/Atlantic region, with land based systems plotted in green and oceanic systems in blue. Flash rate values have been shifted by 0.001 to allow the location of non-flashing systems to be shown on the log-log plot. Black triangles show the mean flash rate for each 1 km bin (including both flashing and non-flashing systems). Also shown are fits of the form  $F = AH^n$  (black lines), with  $A$  and  $n$  values as indicated. Correlation coefficients ( $R$ ) shown on the figure give correlations between observed and fitted values for the individual data points.  $R$  values of 0.97 (storm height) and 0.99 (penetration) occur between the fit and binned data.

**Table 2.** Summary of the Fit Parameters and Regression Coefficients Used for Each Fit Shown in Figure 2<sup>a</sup>

Property	Fit Type	Parameters	R, pA	R, syst
Radar H (single, land)	$A \cdot H_{rad}^n$	$A = 7.67 \times 10^{-5}, n = 4.8$	0.5	0.9
Radar H (single, ocean)	-	-	0.14	0.5
Radar H (L)	$A \cdot H_{rad}^n$	$A = 1.44 \times 10^{-3}, n = 3.5$	0.5	0.9
Radar H (O)	$A \cdot H_{rad}^n$	$A = 3.34 \times 10^{-6}, n = 5.6$	0.13	0.5
Radar H above FL (single, L)	$A \cdot (H_{rad} - H_{fl})^n$	$A = 0.21, n = 1.8$	0.5	0.9
Radar H above FL (single, O)	-	-	0.15	0.45
Radar H above FL (L)	$A \cdot (H_{rad} - H_{fl})^n$	$A = 0.30, n = 1.6$	0.5	0.9
Radar H above FL (O)	$A \cdot (H_{rad} - H_{fl})^n$	$A = 0.04, n = 2.3$	0.12	0.3
Cloud top height (L)	$A \cdot H_{cld}^n$ (per syst)	$A = 9.2 \times 10^{-8}, n = 7.2$	-	0.4
Cloud top height (O)	$A \cdot H_{cld}^n$ (per syst)	$A = 9.1 \times 10^{-10}, n = 7.4$	-	0.24
Rain rate at FL (L)	$A \cdot R_{fl}^n$	$A = 0.039, n = 1.9$	0.2	0.6
Rain rate at FL (O)	$A \cdot R_{fl}^n$	$A = 1.9 \times 10^{-3}, n = 1.3$	0.04	0.25
Deep conv rain frac (L)	$A \cdot Cfrac^n$	$A = 2.72 \times 10^{-3}, n = 1.6$	0.3	0.7
Deep conv rain frac (O)	$A \cdot Cfrac^n$	$A = 9.65 \times 10^{-6}, n = 1.8$	0.17	0.5
Regression (L)	$a + b \cdot H_{cld} + c \cdot H_{cld}^2 + d \cdot H_{cld}^3$ $+ e \cdot R_{fl} + f \cdot Cfrac + g \cdot Cfrac^2$	$a = -8.0, b = 2.25, c = -0.20, d = 5.9 \times 10^{-3},$ $e = 0.14, f = -0.03, g = 6.9 \times 10^{-4}$	0.4	0.7
Regression (O)		$a = -0.55, b = 0.16, c = -0.015, d = 4.7 \times 10^{-4},$ $e = 2.3 \times 10^{-3}, f = 2.3 \times 10^{-3}, g = 3.7 \times 10^{-5}$	0.13	0.4
Regression (single, L)		$a = -4.0, b = 1.27, c = -0.12, d = 3.8 \times 10^{-3},$ $e = 0.11, f = -0.06, g = 9.4 \times 10^{-4}$	0.4	0.8
(single, O)		-	0.16	0.5

<sup>a</sup>Also shown are the correlation coefficients (R) relative to the observed flash rate, both per unit convective area (pA) and per system (syst).

[11] The PR 2A23 rain-type classification (version 6) was used to identify convection, with pixels where the storm height (limit of TRMM sensitivity or  $\sim 17$  dBZ contour) exceeded the height of the  $0^\circ\text{C}$  isotherm considered deep. All systems where PR observes convection were retained in the dataset, with the flash rate per unit area set to zero for systems where none of the convection reaches the freezing level. All warm rain profiles were assumed to be convective in nature, following *Schumacher and Houze* [2003].

[12] The analysis regions are defined in Table 1. For a system to be defined as land or ocean based, the entire cloud anvil must be above the given surface type; otherwise the system is labeled as coastal. We restrict the analysis to tropical regions because midlatitude convection often occurs within synoptic-scale frontal systems rather than convective clusters, and because TRMM sampling of mid-latitudes is poor.

### 3. Results

[13] Figure 1 shows the dependence of the flash rate per unit deep convective area on the average convective storm height and the height above the  $0^\circ\text{C}$  isotherm within the system for the African and Atlantic region. Storm heights are averaged over all convective PR pixels, not only those reaching the  $0^\circ\text{C}$  isotherm or beyond. The use of averaged properties results in a tighter relationship and avoids the quantization of the flash rate values seen in *Ushio et al.* [2001]. Continental and oceanic systems fall roughly along the same line, suggesting that it may be possible to use a single fit in all regions. Separate land and ocean fits return somewhat different coefficients (see Table 2), but do not explain significantly more of the variance. An invariant relationship is not observed for maximum storm heights, which are similar over land and ocean [*Toracinta et al.*, 2002], or if storm heights are only averaged over regions of deep convection.

[14] To fit the dependence of flash rate on storm height, an average value was calculated for each one kilometer bin, including both flashing and non-flashing storms. A least

absolute deviation fit is made to these values, returning a slope,  $n$ , of 4.8, close to the oft cited fifth power law [*Williams*, 1985; *Price and Rind*, 1992] and within the range of values found by *Ushio et al.* [2001].

[15] As mixed-phase microphysics is believed to be essential to the generation of lightning [*Takahashi*, 1978], we also examine the relationship between the flash rate and the height to which radar echoes penetrate above the  $0^\circ\text{C}$  isotherm. *Price and Rind* [1993] previously found that the ratio of cloud to ground flashes depends on this parameter. PR provides a spatially varying estimate of the height of the  $0^\circ\text{C}$  isotherm based on climatological surface temperatures and lapse rates. As can be seen in Figure 1, a power law relationship is again observed, but with a much weaker,  $n \sim 2$ , dependence. Similar behavior ( $n = 1.3$ ) is found when a higher reflectivity threshold of 30 dBZ is used.

[16] To test their predictive capability, both the storm height and  $0^\circ\text{C}$  isotherm penetration based fits developed for the African and Atlantic region are applied to the independent ISCCP based datasets for each of the five regions defined in Table 1. For each system, the observed radar height is used to predict the flash rate per unit area, which is then multiplied by the observed deep convective area to estimate the total number of flashes for that system per minute.

[17] The resulting lightning occurrence and flash rate predictions are summarized in Figure 2. LIS views each region of the earth for about 90 seconds [*Christian*, 1999], giving a minimum detectable flash rate for each system of  $\sim 0.7$  flashes per minute. Systems are therefore defined to have lightning only if the flash rate is greater than this value.

[18] As found by *Boccippio et al.* [2000], both the frequency of occurrence of storms with lightning and flash rates decrease from Africa to the Amazon, maritime continent and ocean regions. Both parameterizations are able to capture this trend, although the echo top height fit overestimates the percentage of storms with lightning in oceanic regions by a factor of four or more. This overestimation can

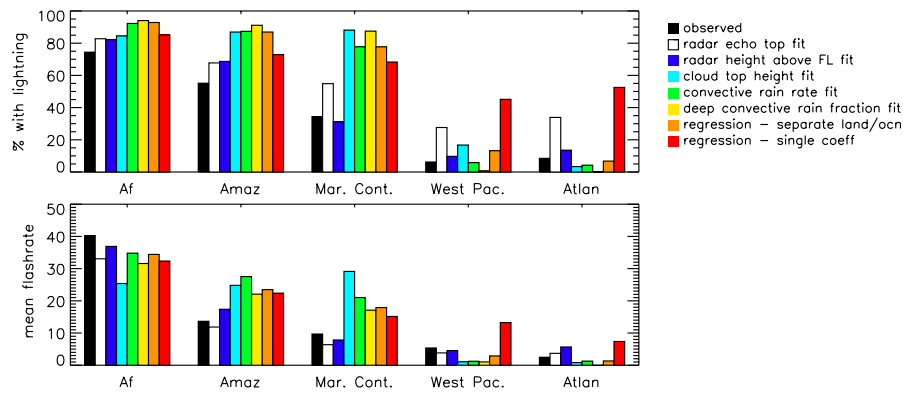


**Figure 2.** Bar charts showing the percentage of systems with lightning (above a flash rate of 0.7 flashes per minute per system) and the mean flash rate (per system per minute) for systems with lightning, for each of the regions listed in Table 1. Observed values are shown in black; results for each fit are colored according to the legend.

be removed by using separate fits over land and ocean (not shown), but at the expense of two additional free parameters. The  $0^{\circ}\text{C}$  isotherm penetration fit performs better, and is able to capture both the land-ocean contrast and the regional differences in lightning occurrence using a single set of parameters. Similar results are found when the 30 dBZ height based fit is used or when the height above a fixed ( $\sim 5$  km) reference level is used. Actual  $0^{\circ}\text{C}$  isotherm heights are nevertheless considered preferable as they allow spatial and seasonal variation in the vertical structure of the atmosphere to be accounted for.

[19] The average height to which large particles penetrate above the  $0^{\circ}\text{C}$  isotherm in regions of convection therefore provides an excellent means to parameterize lightning. However, as many GCMs cannot estimate this quantity, we also investigate the performance of parameterizations based on more widely available quantities including the cloud height, convective rain rate and convective rain fraction. Scatterplots of the flash rate dependence of these properties showing the fits made are provided in Figure S1 of the auxiliary material.<sup>1</sup> As the flash rate per unit area shows only relatively weak dependence on cloud height (not shown), with a stronger relationship observed for the flash rate per system, due to the correlation between system size and depth [Machado and Rossow, 1993], fits were made to the total number of flashes per system in this case. This is consistent with normal application of existing cloud height based algorithms [e.g., Michalon et al., 1999].

[20] The regional and seasonal mean National Centers for Environmental Prediction (NCEP) [Kalnay et al., 1996] temperature profile was used to convert observed brightness temperatures to cloud heights. To avoid errors associated with partial filling at the relatively coarse resolution of the GERB-like data, fits were made to pixel level ( $\sim 5$  km) cloud height estimates from the African/Atlantic region for the summer 2004 ISCCP dataset, although comparisons indicate that this choice has little impact on the overall performance of the parameterization. The system level flash rate shows a roughly seventh order power law dependence on cloud top height over both land and ocean, with a two order of magnitude smaller multiplicative coefficient over

ocean, consistent with observed differences in lightning frequency [Boccippio et al., 2000].

[21] The performance of this fit is shown in Figure 2. While the land-ocean contrast is captured through the use of separate parameterizations, the land fit is unable to capture the observed regional differences. Similar lightning frequencies are predicted for all three regions, with the highest flash rates predicted over the islands of the maritime continent, consistent with the presence of the deepest cloud tops in this region [e.g., Liu et al., 2007]. Similar results are found for the Price and Rind [1992] and Michalon et al. [1999] parameterizations, as shown in Figure S2. No significant improvement in the ability to capture the observed regional contrasts is found using fits to the height of the cloud top above the  $0^{\circ}\text{C}$  isotherm or by fitting the flash rate per unit area (not shown).

[22] Figure 2 also shows results for the power law fits to the dependence of the flash rate per unit area on the  $0^{\circ}\text{C}$  isotherm convective rain rate shown in Figure S1. The decreasing trend in lightning occurrence and flash rates moving from Africa to the maritime continent is captured, but the contrast is much smaller than observed. The fourth order polynomial parameterization proposed by Allen and Pickering [2002] can not be directly compared as it was developed for six hourly, not instantaneous, rain rates, and average values cannot be computed from the ‘snapshot’ TRMM observations.

[23] Power law fits were also made to the dependence of the flash rate per unit convective area on the deep convective rain fraction within the system. Once again, separate fits are required over land and ocean regions and the observed regional differences in lightning occurrence are poorly captured (Figure 2).

[24] The final two bars in Figure 2 correspond to multiple linear regression fits combining information from the cloud height, convective rain rate and convective rain fraction. An iterative approach was used to pick a subset of terms explaining most of the variance (see Table 2). Results in red correspond to the use of a single set of coefficients over both surface types, while those in orange correspond to separate fits to continental and oceanic observations. Use of a single set of coefficients fails to capture the land-ocean contrast, and even when separate fits are used the observed regional differences are poorly captured.

<sup>1</sup>Auxiliary materials are available in the HTML. doi:10.1029/2007GL030227.

[25] The coefficients used for each fit and the correlation coefficients between the fitted and observed flash rates are summarized in Table 2.

#### 4. Discussion and Conclusions

[26] A dataset of convective system properties and flash rate observations are used to investigate relationships between convective cluster properties and lightning flash rates. The fit based on the average height to which radar echoes penetrate above the 0°C isotherm is found to perform best, allowing both the dominant land-ocean contrast in lightning occurrence and regional differences, such as the Africa/Amazon contrast, to be captured using a single approximately second order power law relationship. The variations in flash rate over the system lifecycle observed by FD07 are also well reproduced using this single fit (not shown).

[27] This parameterization is closely linked to our understanding of the physics of lightning production, and has important implications for the sensitivity of lightning to changes in climate. The relatively low order power law implies lower sensitivity than might be inferred from the fifth order dependence for the overall storm height, and suggests that the latter may be an artifact of the need to fit a step change in lightning occurrence as the cloud extends into the mixed phase region. In addition, as only the height of penetration above the freezing level is important, changes in storm height may not result in changes in lightning occurrence if the height of the 0°C isotherm also changes. The use of a single relationship with minimal free parameters which holds in all regions implies a more fundamental physical relationship and removes complexities in parameterizing behaviour in coastal and island regions. Most current GCMs do not make predictions of the large particle top height, but for those that do, a parameterization of the form proposed here can easily be implemented.

[28] Parameterizations based on the cloud top height, convective rain rate and convective rain fraction all require the use of separate fits for land and ocean regions, even when information from multiple variables is combined. These results suggest that parameterization based on the convective rain rate or deep convective rain fraction may perform better than cloud height based fits in capturing regional contrasts over continental regions. However, as GCM predictions of rain rates and rain fractions are highly uncertain [e.g., Dai, 2006] the cloud height based approach may still be preferable.

[29] **Acknowledgments.** TRMM PR data were obtained from the NASA Goddard DAAC, and LIS data from the Global Hydrology Resource Center. ISCCP DX data were obtained from the NASA Langley data center. This research was supported by the NASA Precipitation Measurement Missions Program.

#### References

Allen, D. J., and K. E. Pickering (2002), Evaluation of lightning flash rate parameterizations for use in a global chemical transport model, *J. Geophys. Res.*, *107*(D23), 4711, doi:10.1029/2002JD002066.

Boccippio, D. J., S. J. Goodman, and S. Heckman (2000), Regional differences in tropical lightning distributions, *J. Appl. Meteorol.*, *39*, 2231–2248.

Cecil, D. J., S. J. Goodman, D. J. Boccippio, E. J. Zipser, and S. W. Nesbitt (2005), Three years of TRMM precipitation features. Part I: Radar, radiometric and lightning characteristics, *Mon. Weather Rev.*, *133*, 543–566.

Christian, H. J. (1999), Optical detection of lightning from space, paper presented at 11th International Conference on Atmospheric Electricity, NASA, Guntersville, Ala., 7–11 June.

Dai, A. (2006), Precipitation characteristics in eighteen coupled climate models, *J. Clim.*, *19*, 4605–4630.

Del Genio, A. D., M. S. Yao, and J. Jonas (2007), Will moist convection be stronger in a warmer climate?, *Geophys. Res. Lett.*, doi:10.1029/2006GL030525, in press.

Donner, L. J., C. J. Seman, R. S. Hemler, and S. Fan (2001), A cumulus parameterization including mass fluxes, convective vertical velocities and mesoscale effects: Thermodynamic and hydrological aspects in a general circulation model, *J. Clim.*, *14*, 3444–3463.

Futyán, J. M., and A. D. Del Genio (2007), Deep convective system evolution over Africa and the tropical Atlantic, *J. Clim.*, in press.

Grewe, V., D. Brunner, M. Dameris, J. L. Grenfell, R. Hein, D. Shindell, and J. Staehelin (2001), Origin and variability of upper tropospheric nitrogen oxides and ozone at northern mid-latitudes, *Atmos. Environ.*, *35*, 3421–3433.

Kalnay, E., et al. (1996), The NCEP/NCAR 40-year reanalysis project, *Bull. Am. Meteorol. Soc.*, *77*(3), 437–471.

Liu, C., E. J. Zipser, and S. W. Nesbitt (2007), Global distribution of tropical deep convection: Different perspectives from TRMM infrared and radar data, *J. Clim.*, *20*, 489–503.

Lucas, C., E. J. Zipser, and M. N. LeMone (1994), Vertical velocity in oceanic convection off tropical Australia, *J. Atmos. Sci.*, *51*, 3183–3193.

Machado, L. A. T., and W. B. Rossow (1993), Structural characteristics and radiative properties of tropical cloud clusters, *Mon. Weather Rev.*, *121*, 3234–3260.

Meijer, E. W., P. F. J. van Velthoven, D. W. Brunner, H. Huntrieser, and H. Kelder (2001), Improvement and evaluation of the parameterisation of nitrogen oxide production by lightning, *Phys. Chem. Earth*, *26*(8), 577–583.

Michalon, N., A. Nassif, T. Saouri, J. F. Royer, and C. A. Pontikis (1999), Contribution to the climatological study of lightning, *Geophys. Res. Lett.*, *26*(20), 3097–3100.

Orville, R. E., and R. W. Henderson (1986), Global distribution of midnight lightning: September 1977 to August 1978, *Mon. Weather Rev.*, *114*, 2640–2653.

Price, C., and D. Rind (1992), A simple lightning parameterization for calculating global lightning distributions, *J. Geophys. Res.*, *97*(D9), 9919–9933.

Price, C., and D. Rind (1993), What determines the cloud-to-ground lightning fraction in thunderstorms?, *Geophys. Res. Lett.*, *20*(6), 463–466.

Schumacher, C., and R. A. Houze Jr. (2003), The TRMM Precipitation Radar's view of shallow, isolated rain, *J. Appl. Meteorol.*, *42*, 1519–1524.

Stocks, B. J., et al. (2002), Large forest fires in Canada, 1959–1997, *J. Geophys. Res.*, *107*, 8149, doi:10.1029/2001JD000484. [printed 108(D1), 2003]

Stockwell, D. Z., C. Giannakopoulos, P. H. Plantevin, G. D. Carver, M. P. Chipperfield, K. S. Law, J. A. Pyle, D. E. Shallcross, and K. Y. Wang (1999), Modeling NO<sub>x</sub> from lightning and its impact on global chemical fields, *Atmos. Environ.*, *33*, 4477–4493.

Sud, Y. C., and G. K. Walker (1999), Microphysics of clouds with the relaxed Arakawa-Schubert scheme (McRAS). part I: Design and evaluation with GATE phase III data, *J. Atmos. Sci.*, *56*, 3196–3220.

Takahashi, T. (1978), Riming electrification as a charge generation mechanism in thunderstorms, *J. Atmos. Sci.*, *35*, 1536–1548.

Toracinta, E. R., D. J. Cecil, E. J. Zipser, and S. W. Nesbitt (2002), Radar, passive microwave and lightning characteristics of precipitating systems in the tropics, *Mon. Weather Rev.*, *130*, 802–824.

Ushio, T., S. J. Heckman, D. J. Boccippio, and H. J. Christian (2001), A survey of thunderstorm flash rates compared to cloud top height using TRMM satellite data, *J. Geophys. Res.*, *106*(D20), 24,089–24,095.

Williams, E. R. (1985), Large-scale charge separation in thunderclouds, *J. Geophys. Res.*, *90*(D4), 6013–6025.

Williams, E. R. (2005), Lightning and climate: A review, *Atmos. Res.*, *76*, 272–287.

Williams, E. R., S. A. Rutledge, S. G. Geotis, N. Renno, E. Rasmussen, and T. Rickenbach (1992), A radar and electrical study of tropical “hot towers,” *J. Atmos. Sci.*, *49*, 1386–1395.

Zipser, E. J., and K. R. Lutz (1994), The vertical profile of radar reflectivity of convective cells: A strong indicator of storm intensity and lightning probability?, *Mon. Weather Rev.*, *122*, 1751–1759.

A. D. Del Genio and J. M. Futyán, NASA Goddard Institute for Space Studies, 2880 Broadway, New York, NY 10025, USA. (adelgenio@giss.nasa.gov)